Supporting information

Koeberle et al. 10.1073/pnas.1216182110

SI Materials and Methods

Materials. The following materials were used: nonimmune goat serum (Invitrogen); DMEM/high glucose (4.5 g/L) medium and trypsin/EDTA solution (PAA); sodium vanadate (AppliChem); PGE_2 (Cayman); mouse anti-cyclin D1 (1:2,000), rabbit anti-cyclin B1 (1:1,000), mouse anti-cyclin E antibody (1:1,000), rabbit or mouse anti-β-actin (1:1,000), mouse anti–phospho-ERK1/2 (Thr202/Tyr204; 1:2,000), rabbit anti–phospho-myristoylated alanine-rich C-kinase substrates (MARCKS; Ser152/156; 1:1,000), rabbit anti-caspase 3 (1:1,000), rabbit anti–phospho-Src family (Tyr416; 1:1,000); mouse anti–phospho-JNK (Thr183/Tyr185; 1:2,000), rabbit anti–phospho-p70S6 kinase (Thr389; 1:1,000), rabbit anti–phospho-Akt (Ser473; 1:1,000), rabbit anti–phospho-p38-MAPK (Thr180/Tyr182; 1:1,000), mouse anti-inhibitor of (I)κBα (1:1,000), and rabbit anti–phospho-cytosolic phospholipase A_2 (Ser505, 1:1,000) (Cell Signaling); rabbit anti-Akt (1:500) (Bioss); and goat anti-HSP27 (1:200), rabbit anti–phospho-HSP27 (Ser82; 1:200), and rabbit anti-cytosolic phospholipase A_2 (1:200), (Santa Cruz Biotechnology). Solvents and all other chemicals were obtained from Sigma-Aldrich or Wako Pure Chemicals unless stated otherwise.

Cell Cycle Synchronization with Nocodazole. The concentration of nocodazole has been optimized for the efficiency to enrich cells in the G2/M-phase of the cell cycle (propidium iodide staining and flow cytometry) and for the ability of cells to continue proliferation after withdrawal of nocodazole (light microscopy). Please note that the treatment with nocodazole results in a mixture of diploid and tetraploid cells (four sets of chromosomes instead of two in the G1-phase) as reported for mouse embryonic fibroblasts (1). This mixture results in an apparently increased fraction of cells in the G2/M-phase and less complete progression from the G2/M- to G1-phase, when cell cycle progression was monitored by DNA staining.

Reversed Phase LC and MS. Aqueous ammonium bicarbonate (20 mM) (A) and acetonitrile (B) were used as eluents. The gradient profile was 20–95% B for 20 min and 95% B for 10 min. The flow rate was set to 0.1 mL/min, and the sample volume was 10 μL. Phosphatidylethanolamine (PE) and phosphatidylserine (PS) headgroups were confirmed by $m = 141.0$ or $m = 87.0$ neutral loss scans (collision energy: 25 V; positive and negative ion mode, respectively) and the phosphatidylinositol (PI) headgroup by $m/z = 241.0$ precursor ion scans (collision energy: 35 V; negative ion mode). The fatty acid composition of phospholipids (PLs) was determined from the $[M\text{-}H]^-$ fatty acid anion pattern (single reaction monitoring: collision energy, 40–45 V; product ion scans: m/z 200–400; collision energy, 40–60 V). The isomeric position of the fatty acid in PLs was estimated from the higher signal intensity of *sn*-1 than *sn*-2 fatty acid anions (2). The product ion scans of phosphatidylcholine (PC)(16:0/20:4) standard and cellular PC(16:0/20:4) are compared in Fig. S2*C*. Peaks in extracted mass chromatograms were assigned by manual integration and are baseline corrected. The proportion of lipid species (given as relative intensity) is expressed relative to the sum of all species in the respective subclass (100%) if not indicated otherwise. The relative intensities of isobaric lipid species, which were not separated by LC, were combined for calculation and ascribed to the major lipid species (first mentioned) according to their fatty acid anion profile. Total PL subclass intensities combine the intensities of all species of the respective subclass and were normalized to the number of cells and the internal standard PC(14:0/14:0). Please note that our LC-MS/MS settings and data processing were optimized for the recognition of changes rather than for the determination of absolute lipid masses.

1. Lanni JS, Jacks T (1998) Characterization of the p53-dependent postmitotic checkpoint following spindle disruption. *Mol Cell Biol* 18(2):1055–1064.
2. Hvattum E, Hagelin G, Larsen A (1998) Study of mechanisms involved in the collision-induced dissociation of carboxylate anions from glycerophospholipids using negative ion electrospray tandem quadrupole mass spectrometry. *Rapid Commun Mass Spectrom* 12(19):1405–1409.

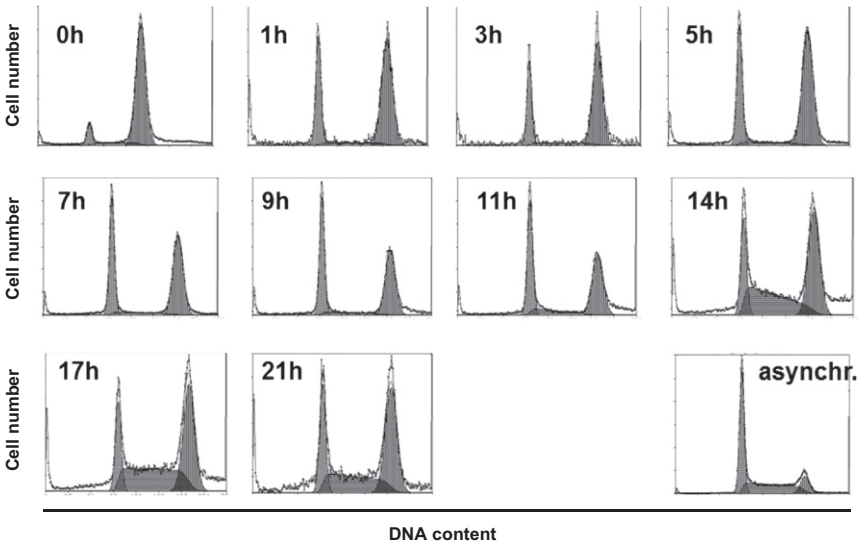

Fig. S1. Cell cycle progression of synchronized NIH 3T3 cells. Cells (4×10^6 cells/10-cm dish) were synchronized by nocodazole (0 h) and released into a new cell cycle. Cell cycle progression was monitored between 0 and 21 h after removal of nocodazole by propidium iodide staining and flow cytometry. Proliferating nontreated cells (asynchr.) were used as control. Histograms are representative of three to six independent experiments.

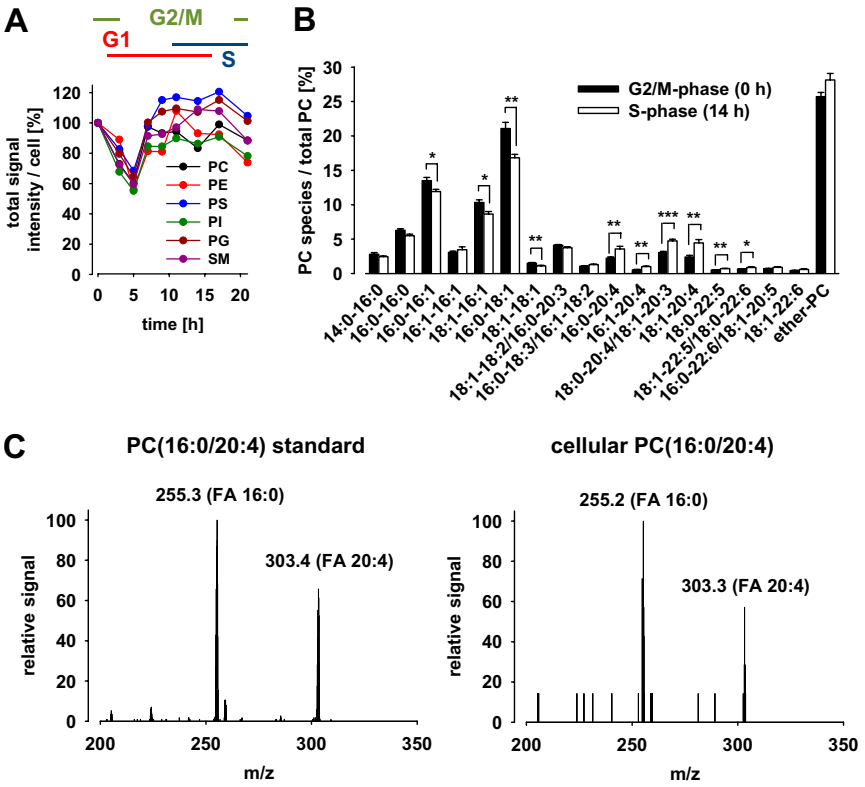

Fig. S2. Cell cycle–dependent changes of the PL profile. NIH 3T3 cells (4×10^6 cells/10-cm dish) were synchronized by nocodazole (0 h) and released into a new cell cycle. (*A*) Time-dependent effect on total PL subclass intensities after removal of nocodazole (0–21 h). Total signal intensities of PL subclasses summarize the relative intensities of individual species and are normalized to the internal standard PC(14:0/14:0) and the number of cells; 100% corresponds to 12.5 ± 1.5 nmol/10^6 cells for PC and is based on relative units for PE, PS, PI, phosphatidylglycerol (PG), and sphingomyelin (SM). (*B*) Relative intensities of individual PC species in the G2/M- and S-phase (0 and 14 h after removal of nocodazole, respectively); 18:3, linolenic acid; 22:5, docosapentaenoic acid; 22:6, docosahexaenoic acid; 20:5, eicosapentaenoic acid; ether-PC, ether-linked PC species. Data are given as means ± SEM; $n = 3$–6. $^*P < 0.05$, $^{**}P < 0.01$, $^{***}P < 0.001$ vs. G2/M-phase (0 h); Student *t* test. (*C*) Product ion scans of PC(16:0/20:4) standard and cellular PC(16:0/20:4) were measured using an Acquity UPLC-coupled QTRAP 5500 mass spectrometer at a collision energy of 60 eV as described in *SI Materials and Methods*. The mass spectrum of the product ion scan (parent mass: $m/z = 782.6$) was averaged over the time window of the peak. The fatty acid anions (FA) are marked.

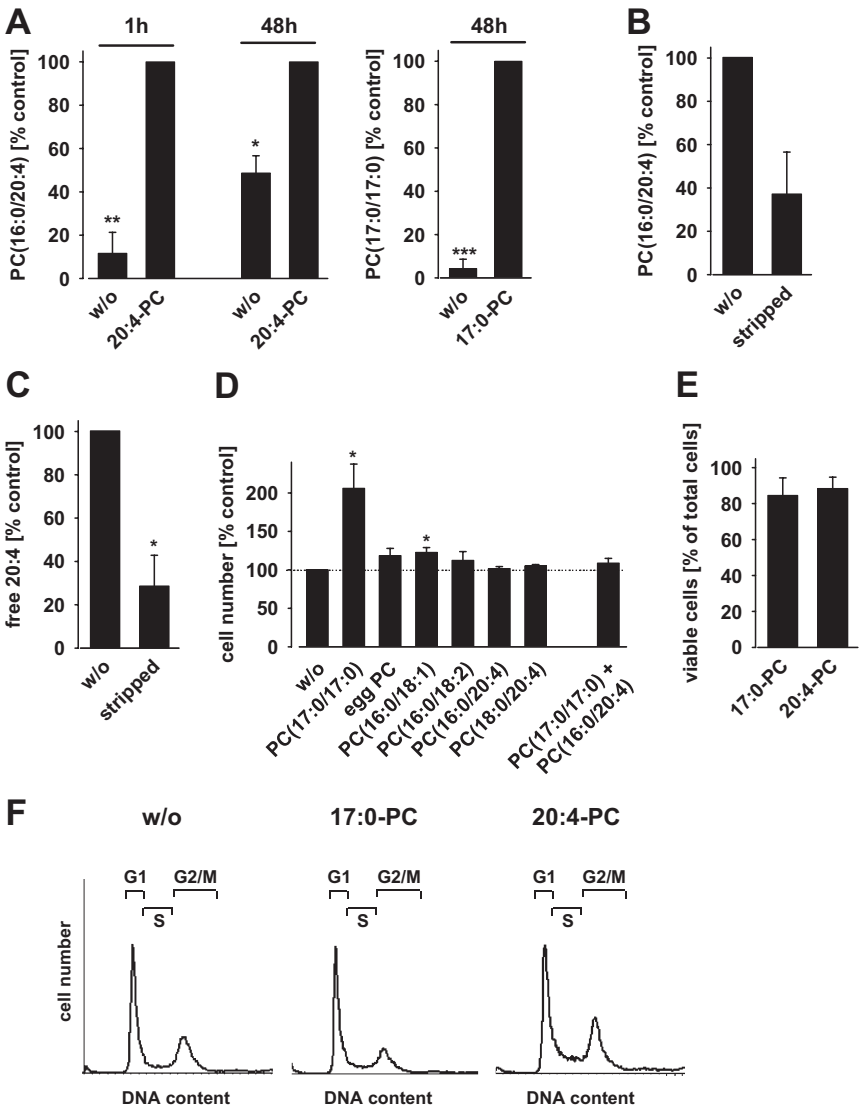

Fig. S3. Supplemented *sn*-2-arachidonoyl-phosphatidylcholine (20:4-PC) is incorporated into NIH 3T3 cells and interferes with cell cycle progression. Cells (1.6×10^4/cm^2) were treated with PC(17:0/17:0) (17:0-PC), PC from egg yolk, PC(16:0/18:1), PC(16:0/18:2), PC(16:0/20:4) (20:4-PC), or PC(18:0/20:4) (120 μM each) in DMEM plus 10% charcoal-stripped FCS. (*A*) After 1 and 48 h, cells (25-cm^2 flask) were washed with PBS, and the amount of cellular PC(16:0/20:4) (20:4-PC) or PC(17:0/17:0) (17:0-PC) was determined by LC-MS/MS. Results are normalized to the internal standard PC(14:0/14:0); 100% corresponds to 8.0 ± 5.8 nmol/10^6 cells (1 h) and 0.9 ± 0.4 nmol/10^6 cells (48 h) PC(16:0/20:4) and 47.2 ± 10.4 nmol/10^6 cells (48 h) PC(17:0/17:0). (*B* and *C*) Signal intensities of PC(16:0/20:4) (*A*) and free 20:4 (*B*) in FCS (w/o) and serum-stripped FCS (stripped) were determined by LC-MS/MS. Signal intensities were normalized to the internal standard PC(14:0/14:0) and the volume of serum; 100% corresponds to 7.2 ± 1.4 nmol PC(16:0/20:4)/mL serum and is based on relative units for free 20:4. (*D* and *E*) Cell numbers (*D*) and cell viability (*E*) were determined after trypan blue staining using a Vi-CELL Series Cell Counter (Beckman Coulter). (*F*) Cell cycle distribution was analyzed by propidium iodide staining and flow cytometry. Representative histograms of three independent experiments are shown. Data are given as means ± SEM; $n = 3$–5. $^*P < 0.05$, $^{**}P < 0.01$, $^{***}P < 0.001$ vs. the 20:4-PC–treated control (*A*) or untreated control (*B*–*D*); Student *t* test.

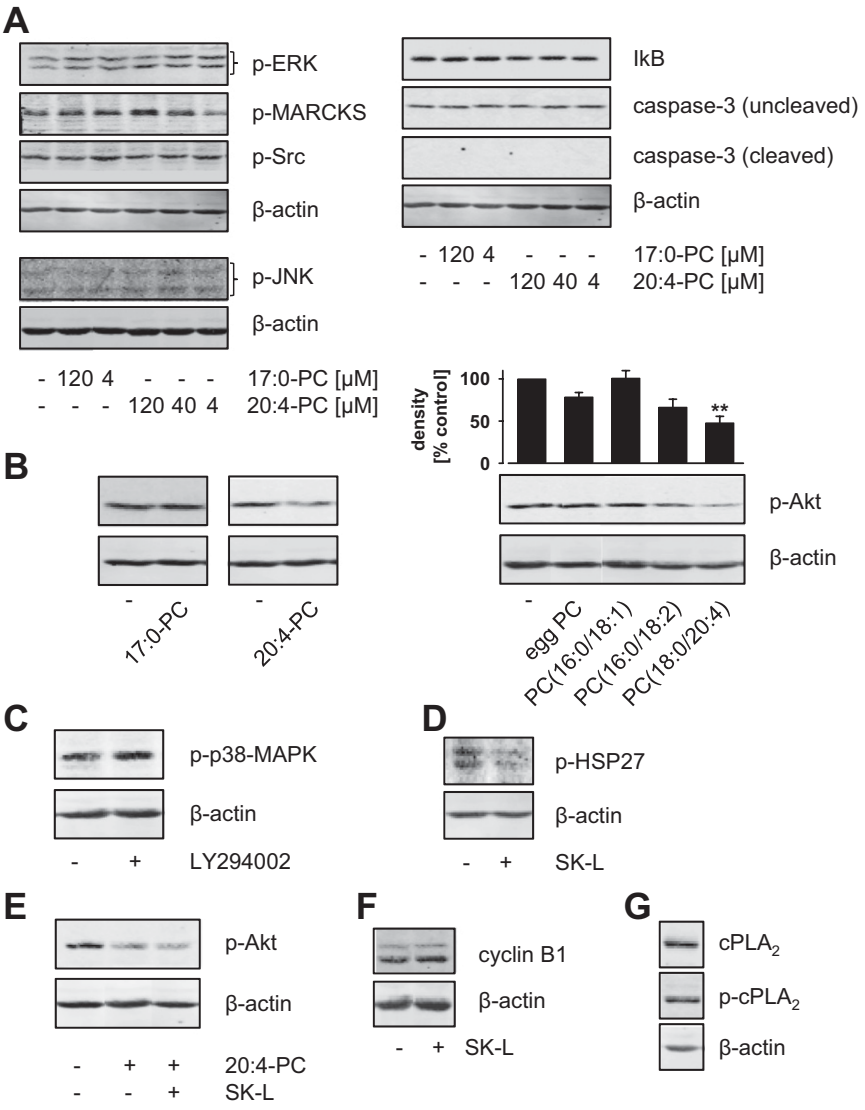

Fig. S4. Effect of 20:4-PC on mitogenic and apoptotic signaling pathways. (*A–C*, *E*, and *F*) NIH 3T3 cells were treated as described in Fig. 2. (*A*) Concentration-dependent effects of PC(17:0/17:0) (17:0-PC) and PC(16:0/20:4) (20:4-PC) on the phosphorylation of ERK1/2 (Thr202/Tyr204), MARCKS (Ser152/156), Src (Tyr416), and p46/p54 JNK (Thr183/Tyr185) and on the expression of the inhibitor of (I)κB and caspase 3 as determined by Western blot. Cleaved caspase-3 was not detectable. (*B*) Effect of PC(17:0/17:0) (17:0-PC), PC(16:0/20:4) (20:4-PC), egg yolk PC, PC(16:0/18:1), PC(16:0/18:2), and PC(18:0/20:4) (120 μM each) on the phosphorylation of Akt (Ser473). β-Actin expression was determined as a control. Data from densitometric analysis are given as means ± SEM; $n = 3$. $^{**}P < 0.01$ vs. the untreated control; ANOVA + Tukey HSD post hoc tests. (*C–F*) Effect of LY294002 (10 μM) and Skepinone-L (SK-L; 0.3 μM) on the phosphorylation of p38-MAPK (Thr180/Tyr182, *C*), HSP27 (Ser82, *D*), and Akt (Ser473, *E*) and on the expression of cyclin B1 (*F*). (*D*) SK-L inhibits p38-MAPK in NIH 3T3 cells. Confluent cells were serum-starved in DMEM plus 0.2% BSA for 24 h. After preincubation with vehicle (DMSO) or the specific p38-MAPK inhibitor SK-L for 10 min, cells were treated with TNFα (15 ng/mL) for 20 min. Phosphorylation of HSP27 (Ser82) was analyzed as marker for p38-MAPK activity. (*G*) Basal protein expression and phosphorylation (Ser505) of cytosolic phospholipase (cPL)A_2 in proliferating NIH 3T3 cells grown in DMEM plus 10% FCS. Western blots are representative of two to four independent experiments.

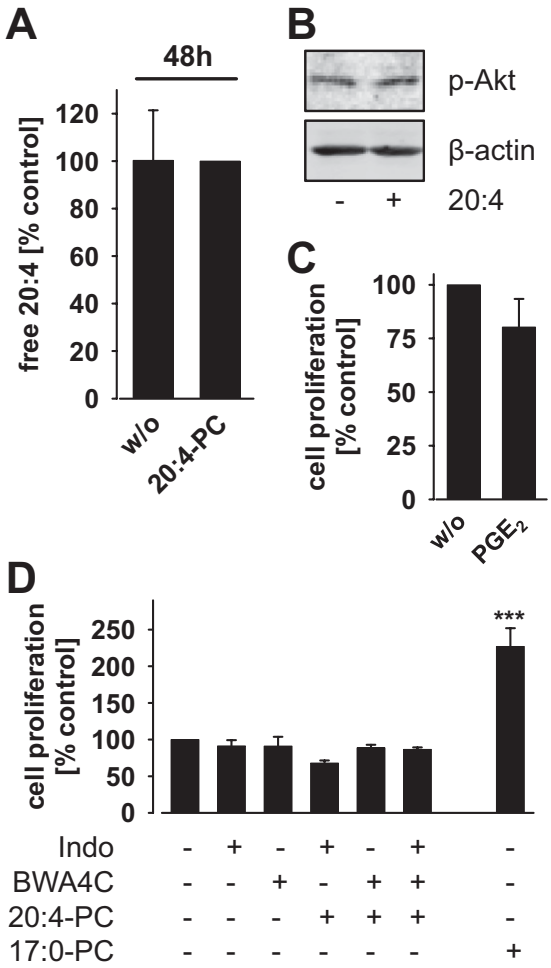

Fig. S5. Effect of 20:4-PC on Akt signaling and proliferation is independent of eicosanoids. (*A* and *B*) Cells (5×10^5/25-cm^2 flask) were treated with PC(16:0/20:4) (120 μM, *A*) or 20:4 (10 μM; *B*) in DMEM plus 10% charcoal-stripped FCS. (*A*) The amount of cellular free 20:4 was determined by LC-MS/MS using single ion monitoring. Results are normalized to the internal standard PC(14:0/14:0); 100% is based on relative units. (*B*) Effect of 20:4 on Akt phosphorylation (Ser473). (*C*) Effect of PGE_2 on cell number. NIH 3T3 cells (5×10^5/25-cm^2 flask) were treated with vehicle (ethanol) or PGE_2 (0.1 μM) for 48 h in DMEM plus 10% FCS. (*D*) The effect of indomethacin (Indo; 10 μM) and BWA4C (1 μM) on cell proliferation was investigated for cells treated with or without PC(16:0/20:4) (20:4-PC, 120 μM) and compared with PC(17:0/17:0) (17:0-PC, 120 μM; Fig. 2*A*). Cells were cultivated for 48 h in DMEM plus 10% charcoal-stripped FCS. Data are given as means ± SEM; $n = 2$–3. ***$P < 0.001$ vs. the untreated control; ANOVA + Tukey HSD post hoc tests.

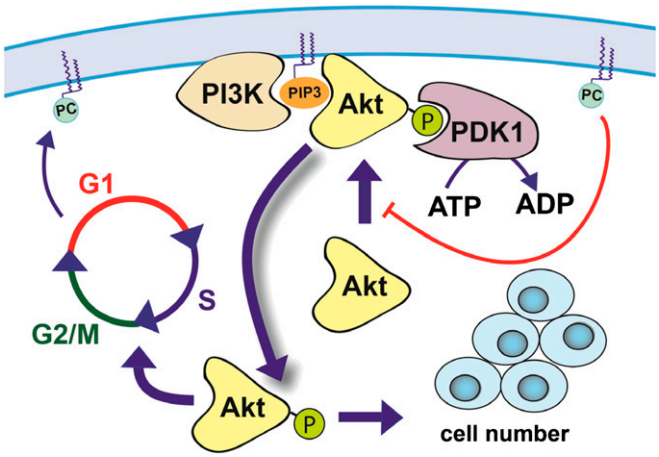

Fig. S6. Schematic overview about the role of 20:4-PC in Akt signaling. The protein kinase Akt binds PIP_3 anchors at membranes. PIP_3 is formed by the receptor-regulated kinase PI3K. Corecruited kinases such as phosphoinositide-dependent protein kinase (PDK)1 activate Akt by phosphorylation. Phosphorylated Akt dissociates from the membrane and activates downstream signaling cascades including p70S6 kinase and cyclins. Akt is a key regulator of cell cycle progression, proliferation, and survival. The ratio of 20:4-PC increases during the G1-phase of the cell cycle and might inhibit Akt membrane translocation and thus activation.

Table S1. Relative intensities of major ether PC species in NIH 3T3 cells

	Relative intensity (% of total PC)	
Ether PC species	G2/M-phase (0 h)	S-phase (14 h)
32:0	2.4 ± 0.1	2.0 ± 0.2*
32:1	6.5 ± 0.1	5.5 ± 0.4
34:2	3.8 ± 0.1	3.1 ± 0.1
36:3	2.0 ± 0.1	1.9 ± 0.1
36:4	2.4 ± 0.2	3.6 ± 0.1**
38:4	2.2 ± 0.1	2.9 ± 0.2
38:5	3.6 ± 0.3	5.4 ± 0.1*
38:6	1.0 ± 0.1	1.2 ± 0.2
40:6	0.9 ± 0.1	1.2 ± 0.0
40:7	0.8 ± 0.1	1.1 ± 0.1

Data are given as means ± SEM; $n = 4–6$.
*$P < 0.05$ and **$P < 0.01$ vs. G2/M-phase; Student t test.